Progress In Electromagnetics Research, Vol. 135, 201–213, 2013

A SUBSTRATE INTEGRATED WAVEGUIDE BANDPASS FILTER USING NOVEL DEFECTED GROUND STRUCTURE SHAPE

Yongmao Huang[1], Zhenhai Shao[1, 2, *], and Lianfu Liu[1]

[1]School of Communication and Information Engineering, University of Electronics Science and Technology of China, Chengdu 611731, China

[2]State Key Laboratory of Millimeter Waves, Southeast University, Nanjing 210096, China

Abstract—In this paper, a X-band wideband bandpass filter based on a novel substrate integrated waveguide-to-defected ground structure (SIW-DGS) cell is presented. In the cell, the DGS is etched on the top plane of the SIW with high accuracy, so that the performance of the filter can be kept as good as possible. Finally, the filter, consisting of three cascaded cells, is designed and measured to meet compact size, low insertion loss, good return loss as well as smooth group delay. There is good agreement between the measurement and simulation results.

1. INTRODUCTION

Substrate integrated waveguide (SIW), early introduced by *Wu* et al., has attracted plenty of attention and utilized in different applications due to its merits of higher quality factor, easy integration, low cost, high power handling and mass production [1–5]. The half-mode substrate integrated waveguide (HMSIW) has been developed for microwave and millimeter wave applications [6, 7]. The HMSIW gave good performance and almost 50% reduction in SIW size. However, compared with the microstrip circuitry, the conventional rectangular cavity resonator of the HMSIW is still too large to make its physical size be small enough.

In order to reduce the size of SIW components, several technologies have been proposed. The first one is to utilize the multilayer low temperature co-fired ceramic (LTCC) and printed

Received 4 November 2012, Accepted 14 December 2012, Scheduled 19 December 2012

* Corresponding author: Zhenhai Shao (shao_zh@uestc.edu.cn).

circuit board (PCB) process to develop the three dimensional substrate integrated circular and elliptic cavity (3D SICC and SIEC) [8–10] and the folded substrate integrated waveguide [11, 12]. It can make the SIW cavities to be folded and to couple with each other in the vertical direction, so that the component's size can be reduced greatly. However, size-reducing in this method is at the cost of fabrication complexity and cost. The second method to do size-miniaturization is to use metamaterial resonators, such as the complementary split ring resonator (CSRR) [13], the complementary sprial resonator (CSR) [14] and the composite right/left-handed structures (CRLH) [15], which exhibit negative permittivity and permeability. As they are utilized in the SIW, a passband propagation below its cut-off frequency of the dominant mode can be achieved. However, it is quite unacceptable in microwave and millimeter wave applications that the measured insertion losses of all experimental filters in [13, 14] are not low enough. Another promising approach is the defected ground structure (DGS), which is etched as featured patterns in the ground plane of planar circuit board to change the ground current distribution and generate resonance, so as to increase stopband reduction and reduce size of the circuit [16–19]. However, since all DGS referred above are etched into the bottom side of the circuit boards, it is inconvenient to integrate them with other components in one metallic cavity. Solution for this drawback is to etch DGS in the plane of signal transmission lines of the coplanar waveguide (CPW) [20, 21] and SIW [22].

2. ANALYSIS OF SIW-DGS CELL

The proposed SIW-DGS cell is shown in Figure 1. Since the DGS is etched into the top metal cover of SIW, it is quite convenient to do system integration. For this proposed SIW-DGS cell, its bandpass function is the composite high-low (Hi-Lo) type, i.e., it is a combination of the highpass guided wave function of SIW and the bandgap function of DGS.

As discussed in [1, 2], the characteristic cutoff frequency of the SIW is mainly controlled by its width a in Figure 1. A SIW with a and h, the height of the substrate, can be equivalent to a conventional rectangular waveguide with the same height, h, and width, $a_{\text{EFF\_SIW}}$, which is shown as

$$a_{\text{EFF\_SIW}} = a - \frac{(2R)^2}{0.95D}, \tag{1}$$

where R and D are the vias' radius and the spacing between two adjacent vias, respectively. As shown in [1], the Equation (1) is valid for $D < \lambda_0\sqrt{\varepsilon_r/2}$ and $D < 8R$ within $\pm 5\%$ precision, where λ_0 and

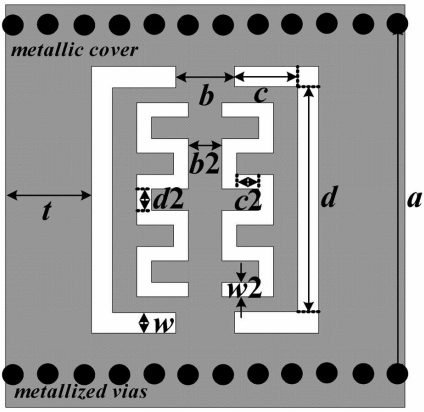

Figure 1. Proposed SIW-DGS cell (top layer).

ε_r are the wavelength in free space and the relative permittivity of the substrate, respectively. As R increases, the small error will appear, which has been discussed in [23]. To improve the precision, a more accurate width $a_{\text{EFF\_SIW}}$ can be rewritten as

$$a'_{\text{EFF\_SIW}} = a - 1.08\frac{(2R)^2}{D} + 0.1\frac{(2R)^2}{a}, \tag{2}$$

where good precision can be obtained under conditions of $D/(2R) < 3$ and $a/R > 5$, which has been reported in [23]. To make the effect of D to be more intuitive, some simulated results of one SIW with different D is given in Figure 2, where the relative permittivity $\varepsilon_r = 2.2$, $a = 7.0\,\text{mm}$, $h = 0.508\,\text{mm}$, and $R = 0.25\,\text{mm}$. According to Figure 2(a), as D increases, although the cutoff frequency almost has no change, the rejection under the cutoff frequency improve greatly, which is a positive influence. However, the negative influence is the return loss in the passband becomes worse with the increasing of D. Furthermore, as shown in Figure 2(b), the insertion loss in the passband increases from 0.12 dB to over 0.16 dB as D increases from 0.8 mm to 1.2 mm. This may be due to the fact that energy leakage increase with increasing $D/(2R)$.

In this SIW-DGS cell, the upper cutoff frequency is mainly controlled by the DGS. For proposed DGS shape, size of its slots and the spacing between adjacent slots are very important parameters to affect the bandgap point and the bandgap strength. To make the characteristics of proposed DGS clear, these parameters are discussed in details, with the same conditions as $\varepsilon_r = 2.2$, $a = 7.0\,\text{mm}$, $h = 0.508\,\text{mm}$, $R = 0.25\,\text{mm}$, and $D = 1\,\text{mm}$. The influence of the

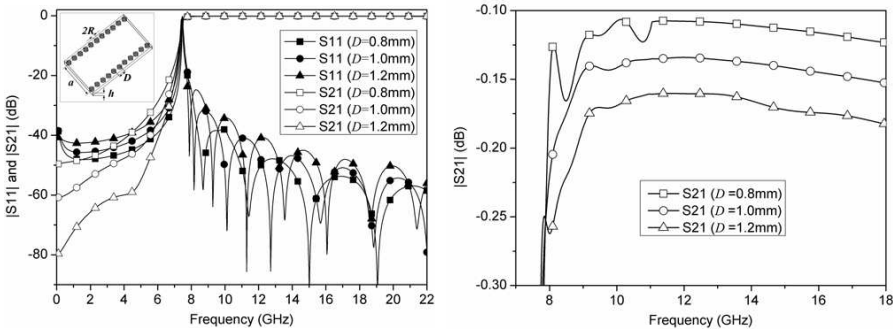

Figure 2. Simulated results of SIW with different values of D. (a) S-parameters within a wide frequency range, (b) difference of insertion loss in the interested passband.

outer slots' size is simulated and shown in Figure 3. It can be found that as c or d increases, i.e., size of the outer slots gets larger, the upper cutoff frequency and bandgap point shifts lower, while the lower cutoff frequency nearly keeps the same. That means the larger the size of the DGS is, the lower the bandgap frequency is. On one hand, for the same d, the longer c is, the stronger the bandgap strength is. Inversely, for the same c, as d gets longer, the bandgap strength gets weaker. For different group choosing of c and d with "$2c+d = 7.0\,\text{mm}$", such as "$c = 1.25\,\text{mm}$, $d = 4.5\,\text{mm}$", "$c = 1.00\,\text{mm}$, $d = 5.0\,\text{mm}$" and "$c = 0.75\,\text{mm}$, $d = 5.5\,\text{mm}$", it can be seen that the longer c is, the lower the upper cutoff frequency and the bandgap point are, and the stronger the bandgap strength is. As shown in Figure 3, the bandgap strength of "$c = 1.25\,\text{mm}$, $d = 4.5\,\text{mm}$" is over 60 dB, which is much stronger than those of "$c = 1.00\,\text{mm}$, $d = 5.0\,\text{mm}$" and "$c = 0.75\,\text{mm}$, $d = 5.5\,\text{mm}$". In a components design using this SIW-DGS cell, the lengths of c and d should be tradeoff and tuned to meet the design requirement.

For the inner slow-wave slots, their sizes, mainly determined by the transverse length $c2$ and longitudinal length $d2$, have little influence on the passband transmission characteristics, but can affect the upper stopband performance heavily. According to Figure 4, for the same $d2$, as $c2$ gets longer, the transmission characteristics nearly have no change in the passband, and only have a very small difference in the bandgap point. But for the same $c2$, as $d2$ gets longer, the upper stopband transmission behavior gets worse rapidly and heavily. As shown in Figure 4, when $d2$ increases from 0.3 mm to 0.6 mm, lots of

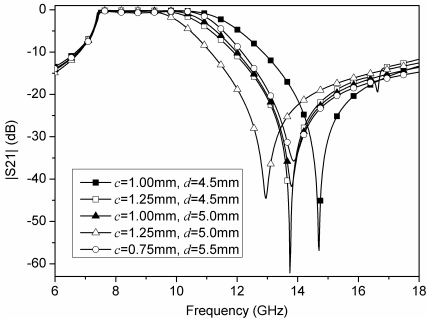

Figure 3. Simulated results of proposed SIW-DGS cell with different values of c and d, where $b = 1.5\,\text{mm}$, $b2 = 0.5\,\text{mm}$, $c2 = d2 = 0.3\,\text{mm}$, $w = 0.5\,\text{mm}$ and $w2 = 0.3\,\text{mm}$.

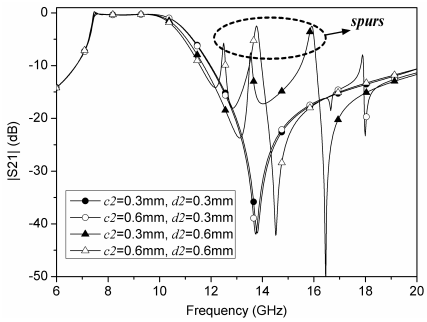

Figure 4. Simulated results of proposed SIW-DGS cell with different values of $c2$ and $d2$, where $b = 1.5\,\text{mm}$, $w = 0.5\,\text{mm}$, $w2 = 0.3\,\text{mm}$, $c = 1.0\,\text{mm}$ and $d = 5.0\,\text{mm}$.

spurs occur in the stopband, which is unacceptable in filter design. So when this cell is used in the design, the longitudinal length of the slow-wave slots should be tuned to reach a good stopband spurious performance.

Figure 5 shows the simulated results of the proposed SIW-DGS cell with different spacing of the two outer slots, i.e., b. It can be seen that as b gets wider, the upper cutoff frequency of proposed cell shifts lower, but the bandgap point shifts higher, which means that the upper skirt selectivity gets worse and that the bandwidth gets narrower. The bandgap strength of "$b = 2.0\,\text{mm}$" is much stronger than those of "$b = 1.0\,\text{mm}$" and "$b = 3.0\,\text{mm}$". As "$b = 3.0\,\text{mm}$", spur occurs in the stopband. So it can be predicted that there is an optimal value of "b" around 1.0 mm to 2.0 mm, which can help to optimize the performance in components design.

3. FILTER DESIGN

Based on the proposed SIW-DGS cell, a X-band wideband bandpass filter is designed. In this filter design, two elements are pivotal: one is the identical property of the SIW-DGS cell, which has been presented exhaustively in Section 2, and the other is the cascade of two adjacent cells. In the cascade of two cells, "s", width of the metal spacing between them, is the decisive factor to affect the transmission characteristics, such as the upper skirt selectivity, the spur's location and its strength. As shown in Figure 6, the wider the spacing is, the

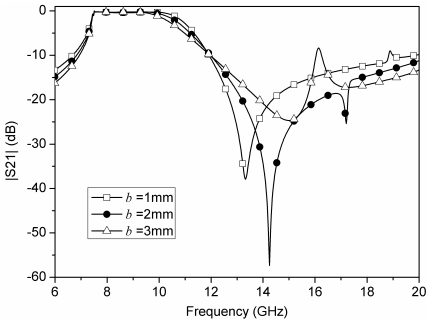

Figure 5. Simulated results of proposed SIW-DGS cell with different values of b, where $c = 1.0\,\text{mm}$, $d = 5.0\,\text{mm}$, $w = 0.5\,\text{mm}$, $w2 = 0.3\,\text{mm}$ and $c2 = d2 = 0.3\,\text{mm}$.

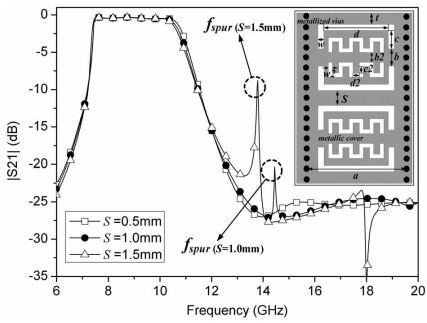

Figure 6. Simulated results of the cascading of two cells with different values of "s", where $b = 1.5\,\text{mm}$, $c = 1.0\,\text{mm}$, $d = 5.0\,\text{mm}$, $w = 0.5\,\text{mm}$, $w2 = 0.3\,\text{mm}$ and $c2 = d2 = 0.3\,\text{mm}$.

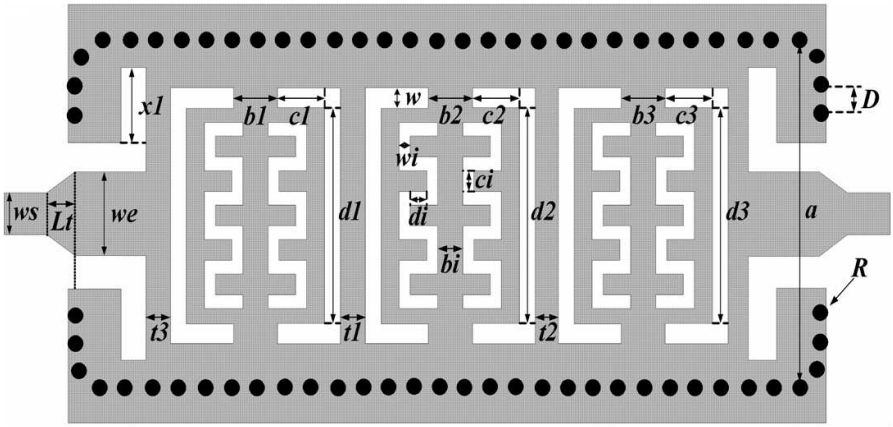

Figure 7. Configuration of proposed filter with three cascaded SIW-DGS cells.

worse the skirt selectivity is, the lower the spur occurs and the stronger its strength is.

The configuration of proposed filter is shown in Figure 7. It consists of three cascaded cells in the middle and two CPW-SIW transitions at input/output (I/O) ports in order to achieve high external quality factor. Its optimized dimensions and electric field distribution are demonstrated in Table 1 and Figure 8, respectively. According to its electric field distribution, most of the energy is

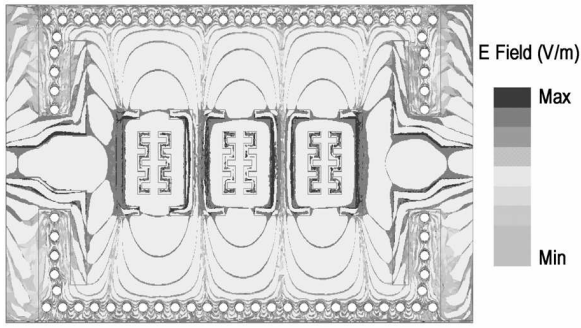

Figure 8. Electric field distribution of proposed filter with three cascaded SIW-DGS cells.

Table 1. Dimensions of proposed filter with three cascaded SIW-DGS cells.

Symbol	Quality (mm)	Symbol	Quality (mm)
ws	1.52	$b1$	2
w	0.5	$c1$	1
a	14.8	$d1$	4.65
wi	0.3	$t1$	0.52
Lt	1.1	$b2$	2.1
D	1	$c2$	0.95
R	0.25	$d2$	4.7
bi	0.6	$t2$	0.49
we	2.6	$b3$	2
$x2$	3.8	$c3$	1.05
di	0.25	$d3$	4.6
ci	0.3	$t3$	1.8

restrained in the DGS slots, so that most of the transmission can be carried out around the slots, which can reduce the transmission loss resulted from the coupling aperture in conventional cavity filter.

4. EXPERIMENTAL RESULTS

Using a single layer PCB process, the filter, as shown in Figure 9, is fabricated on a RT/Duroid 5880 substrate with relative permittivity of 2.2 ± 0.02, loss tangent 0.001 (at 10 GHz) and a thickness of 0.508 mm,

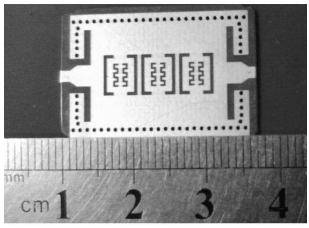

Figure 9. Photograph of fabricated filter with three cascaded SIW-DGS cells.

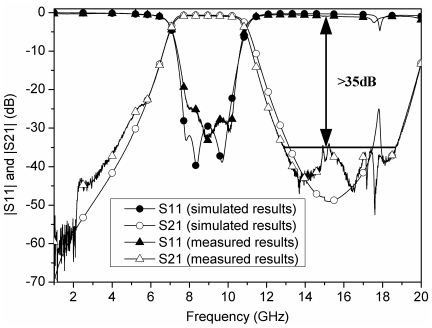

Figure 10. Comparison of measured and simulated results.

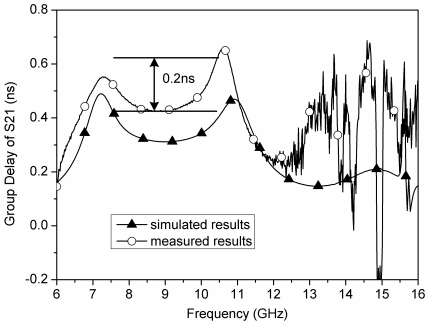

Figure 11. Measured and simulated group delay of S_{21}.

and is measured by the Agilent Vector Network Analyzer N5245A. Its simulated and measured S-parameters are compared in Figure 10. From the measured results, the filter has a central frequency of 9 GHz, a fractional bandwidth of 32% and return loss better than 20 dB in the whole passband. The measured maximum insertion loss is 0.81 dB, about 0.15 dB worse than that of the simulated one, and the ripple in the passband is less than 0.2 dB. As shown in Figure 10, the measured upper 3-dB cutoff frequency is a bit lower than that of the simulated one, which might be caused by the variation of substrate's permittivity and the inaccuracy in fabrication. In Figure 11, whatever for measured and simulated results, both variations of the group delay of S_{21} are less than 0.2 ns, which is quite smooth for a microwave filter. So, the proposed filter can be used as a linear phase filter in broadband wireless communication and digital microwave system.

To inspect the performance of proposed filter clearer, some comparisons between the proposed filter and several previous SIW cavity filters, folded SIW filter and SIW-DGS filters reported in the references are summarized in Table 2. According to the comparisons,

Table 2. Comparison with filters presented in references.

Reference filter	Order	Topology	Central frequency and fractional bandwidth
[6]	3	HMSIW- Slot	7.8 GHz and 22%
[9]	2	3D SICC	10.05GHz and 3.3%
[10]	2	3D SICC/SIEC	10.03 GHz and 3.4%
[12]	4	HMSIFW	9.9725 GHz and 0.8%
[22]	3	SIW-CSRR	8.15 GHz and 23%
[24]	3	SIW cavity	10.09 GHz and 3%
[25]	3	CSRR cavity	5.03 GHz and 6.4%
[26]-1	3	SIW-EBG	13GHz and 46.1%
[26]-2	3	SIW-DGS (bottom)	11.75 GHz and 55.32%
[26]-3	3	SIW-CPW	11.75 GHz and 55.32%
[27]	3	SIFW	10 GHz and 1%
[28]	3	SIW-CSRR (bottom)	9.4 GHz and 30%
[29]	4	7.8 GHz and 6%	Folded SIW
Proposed	3	SIW-DGS	9 GHz and 32%
Reference filter	Insertion loss (dB)	Return loss (dB)	Size (λ_0^2)
[6]	1.5	> 10	> 0.20
[9]	1.9	> 18.5	> 0.54
[10]	1.65	> 19.5	> 0.53
[12]	1.5	> 12	> 0.47
[22]	2.16	11.6	0.35
[24]	3.13	> 13.5	1.49
[25]	3.9	> 19	0.58
[26]-1	$2.5 \sim 5$	> 10	0.39
[26]-2	> 1.4	> 11	> 0.26
[26]-3	> 0.8	> 11	> 0.25
[27]	2.7	> 20	0.65
[28]	1	16	0.47
[29]	2.62	> 10	0.15
Proposed	< 0.81	> 20	0.36

although the return losses of the filters in [24, 25] are quite good, their insertion losses are much higher than that of the proposed one, which is mainly contributed by the transmission loss of inter-coupling between

adjacent cavities and the radiation loss. Compared with the proposed filter, due to the narrow band, the cross-layer aperture coupling and multilayered structure, the multilayered filters reported in [9, 10, 12, 27] have higher insertion loss, larger sizes and higher fabrication price. Although the SIW-DGS filter in [26]-2 and the SIW-CSRR filter in [28] have good performance on the whole, as a tradeoff of insertion loss, return loss and size, they are inconvenient to do system integration owing to their DGS and CSRR etched into the bottom metal cover. Although the SIW-CPW filter in [26]-3 is with compact size, low insertion loss and is easy to do system integration, its return loss is not so good as well as the in-band ripple of its insertion loss is over 0.5 dB, which is much larger than that of the proposed one. This larger ripple will make the error vector magnitude (EVM) of the signal to be much worse when such kind of filter is used in the digital microwave system with high-order quadrature amplitude modulation (QAM). It is obvious that the proposed filter can achieve lower insertion loss, better return loss and more compact size on the whole. Comparison of the group delay of S_{21} is not available here because most of the filters presented in references haven't been reported.

5. CONCLUSIONS

A X-band wideband bandpass filter based on the novel SIW-DGS cell is designed, fabricated, and measured. The measured results are in good agreement with the simulated one in group delay, in-band ripple and linear-like phase. Compared with some reported filters operating at similar frequency, the proposed filter has better overall performance in insertion loss, return loss and size.

ACKNOWLEDGMENT

This work was supported in part by Greating Technology (Beijing) Co. Ltd. and in part by Foundation of State Key Laboratory of Millimeter Wave, Southeast University, under Grant No. K201111.

REFERENCES

1. Cassivi, Y., L. Perregrini, P. Arcioni, M. Bressan, K. Wu, and G. Conciauro, "Dispersion characteristics of substrate integrated rectangular waveguide," *IEEE Microw. Wirel. Compon. Lett.*, Vol. 12, No. 9, 333–335, Sep. 2002.
2. Deslandes, D. and K. Wu, "Accurate modeling, wave mechanism, and design consideration of a substrate integrated waveguide,"

IEEE Trans. on Microw. Theory and Tech., Vol. 54, No. 6, 2516–2526, Jun. 2006.

3. Djerafi, T., N. J. G. Fonseca, and K. Wu, "Design and implementation of a planar 4×4 Butler Matrix in SIW technology for wide band high power applications," *Progress In Electromagnetics Research B*, Vol. 35, 29–51, 2011.
4. Cheng, Y. J., "Substrate integrated waveguide frequency-agile slot antenna and its multibeam application," *Progress In Electromagnetics Research*, Vol. 130, 153–168, 2012.
5. Su, P., Z.-X. Tang, and B. Zhang, "Push-push dielectric resonator oscillator using substrate integrated waveguide power combiner," *Progress In Electromagnetics Research Letters*, Vol. 30, 105–113, 2012.
6. Wang, Y. Q., W. Hong, Y. D. Dong, B. Liu, H. J. Tang, J. X. Chen, X. X. Yin, and K. Wu, "Half mode substrate integrated waveguide (HMSIW) bandpass filter," *IEEE Microw. Wirel. Compon. Lett.*, Vol. 17, No. 4, 265–267, Apr. 2007.
7. Song, Q. Y., H. R. Cheng, X. H. Wang, L. Xu, X. Q. Chen, and X. W. Shi, "Novel wideband bandpass filter integrating HMSIW and DGS," *Journal of Electromagnetic Waves and Applications*, Vol. 23, Nos. 14–15, 2031–2040, 2009.
8. Gu, J., Y. Fan, and Y. Zhang, "A X-band 3-D SICC filter with low-loss and narrow band using LTCC technology," *Journal of Electromagnetic Waves and Applications*, Vol. 23, Nos. 8–9, 1093–1100, 2009.
9. Zhang, Z. G., Y. Fan, Y. J. Cheng, and Y.-H. Zhang, "A compact multilayer dual-mode substrate integrated circular cavity (SICC) filter for X-band application," *Progress In Electromagnetics Research*, Vol. 122, 453–465, 2012.
10. Zhang, Z. G., Y. Fan, Y. J. Cheng, and Y.-H. Zhang, "A novel multilayer dual-mode substrate integrated waveguide complementary filter with circular and elliptic cavities (SICC and SIEC)," *Progress In Electromagnetics Research*, Vol. 127, 173–188, 2012.
11. Wang, R., L.-S. Wu, and X.-L. Zhou, "Compact folded substrate integrated waveguide cavities and bandpass filter," *Progress In Electromagnetics Research*, Vol. 84, 135–147, 2008.
12. Wang, Z., X. Li, S. Zhou, B. Yan, R.-M. Xu, and W. Lin, "Half mode substrate integrated folded waveguide (HMSIFW) and partial H-plane bandpass filter," *Progress In Electromagnetics Research*, Vol. 101, 203–216, 2010.

13. Dong, Y.-D., T. Yang, and T. Itoh, "Substrate integrated waveguide loaded by complementary split-ring resonators and its applications to miniaturized waveguide filters," *IEEE Trans. on Microw. Theory and Tech.*, Vol. 57, No. 9, 2211–2223, Sep. 2009.
14. Zhou, L., S. Liu, N. Gao, Y. Chen, and Y. Wei, "Miniaturized substrate integrated waveguide filter with complementary sprial resonator," *Microwave and Optical Technology Letters*, Vol. 53, No. 6, 1308–1311, Jun. 2011.
15. Dong, Y.-D. and T. Itoh, "Composite right/left-handed substrate integrated waveguide and half-mode substrate integrated waveguide," *Proc. IEEE MTT-S International Microwave Symposium Digest*, 49–52, Jun. 2009.
16. Ahn, D., J.-S. Park, C.-S. Kim, J. Kim, Y.-X. Qian, and T. Itoh, "A design of the low-pass filter using the novel microstrip defected ground structure," *IEEE Trans. on Microw. Theory and Tech.*, Vol. 49, No. 1, 86–93, Jan. 2001.
17. Chen, J., Z.-B. Weng, Y.-C. Jiao, and F.-S. Zhang, "Lowpass filter design of Hilbert curve ring defected ground structure," *Progress In Electromagnetics Research*, Vol. 70, 269–280, 2007.
18. Sheta, A. F., "A novel compact degenerate dual-mode square patch filter using cross H-shaped defected ground structure," *Journal of Electromagnetic Waves and Applications*, Vol. 22, Nos. 14–15, 1913–1923, 2008.
19. Gupta, N., P. Ghosh, and M. Toppo, "A miniaturized Wilkinson power divider using DGS and fractal structure for GSM application," *Progress In Electromagnetics Research Letters*, Vol. 27, 25–31, 2011.
20. Shao, Z. H. and M. Fujise, "Bandpass filter design based on LTCC and DGS," *17th Asia-Pacific Microwave Conference*, 138–139, 2005.
21. Ke, P.-Y., H.-C. Chiu, F.-H. Huang, H.-L. Kao, and Q. Xue, "Characterization of compact V-band GaAs CMRC filter using slow wave CPW transmission lines technology," *Progress In Electromagnetics Research B*, Vol. 43, 355–372, 2012.
22. Zhang, X.-C., Z.-Y. Yu, and J. Xu, "Novel band-pass substrate integrated waveguide (SIW) filter based on complementary split ring resonators (CSRR)," *Progress In Electromagnetics Research*, Vol. 72, 39–46, 2007.
23. Xu, F. and K. Wu, "Guided-wave and leakage characteristics of substrate integrated waveguide," *IEEE Trans. on Microw. Theory and Tech.*, Vol. 53, No. 1, 66–73, Jan. 2005.

24. Ismail, A., M. S. Razalli, M. A. Mahdi, R. S. A. R. Abdullah, N. K. Noordin, and M. F. A. Rasid, "X-band trisection substrate-integrated waveguide quasi-elliptic filter," *Progress In Electromagnetics Research*, Vol. 85, 133–145, 2008.
25. Jiang, W., W. Shen, L. Zhou, and W.-Y. Yin, "Miniaturized and high-selectivity substrate integrated waveguide (SIW) bandpass filter loaded by complementary split-ring resonators (CSRRs)," *Journal of Electromagnetic Waves and Applications*, Vol. 26, Nos. 11–12, 1448–1459, Aug. 2010.
26. Hao, Z.-C., W. Hong, J.-X. Chen, X.-P. Chen, and K. Wu, "Compact super-wide bandpass substrate integrated waveguide (SIW) filters," *IEEE Trans. on Microw. Theory and Tech.*, Vol. 53, No. 9, 2968–2977, Sep. 2005.
27. Wang, Z., D. Shen, R. Xu, B. Yan, and W. Lin, "A partial H-plane substrate integrated folded waveguide (SIFW) bandpass filter based on H-plane slot," *Journal of Electromagnetic Waves and Applications*, Vol. 24, No. 1, 113–121, 2010.
28. Deng, K., Z. Guo, C. Li, and W. Che, "A compact planar bandpass filter with wide out-of-band rejection implemented by substrate-integrated waveguide and complementary split-ring resonator," *Microwave and Optical Technology Letters*, Vol. 53, No. 7, 1483–1487, Jul. 2011.
29. Wang, R., L.-S. Wu, and X.-L. Zhou, "Compact folded substrate integrated waveguide cavities and bandpass filter," *Progress In Electromagnetics Research*, Vol. 84, 135–147, 2008.